

March
2010
No. 36

CONFOCAL APPLICATION LETTER



reSOLUTION

Fluorescence Correlation Spectroscopy :
The Femtoliter Test Tube –
System Calibration and *In Vitro* Applications

Leica
MICROSYSTEMS

This application letter explains

- The principle of fluorescence correlation spectroscopy
- System calibration
- Step-by-step guide for the implementation of an FCS experiment using a Leica TCS SMD System
- Step-by-step guide for curve fitting using Picoquant's SymPhoTime software
- How to avoid common artefacts, like detector afterpulsing, photobleaching, optical saturation and molecular dark states

Fig. 1 Observation volume and important parameters. The diffusion time τ_D indicates the time molecules spend within the observation volume, i.e. how long it takes to diffuse laterally. The lateral extension (beam waist), w_0 , and the axial extension, z_0 , of the observation volume are given (right hand side). Their ratio z_0/w_0 is the eccentricity or structure parameter, κ .

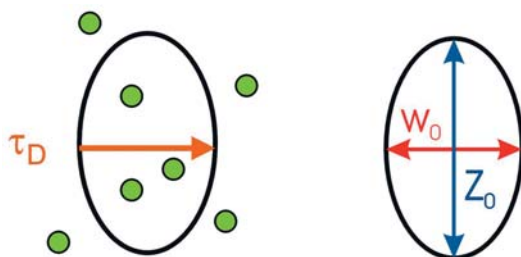
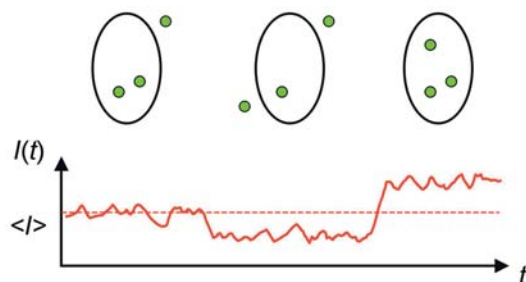


Fig. 2 Fluorescence intensity trace. Movement of molecules into and out of the observation volume (upper row) leads to random fluctuations of fluorescence intensity.



FCS – The Principle

Fluorescence correlation spectroscopy (FCS) measures fluctuations of fluorescence intensity in a sub-femtolitre volume to detect such parameters as the diffusion time, number of molecules or dark states of fluorescently labeled molecules. The technique was independently developed by Watt Webb and Rudolf Rigler during the early 1970s. The term FCS was coined by the Webb lab [1]. The breakthrough of the technique was the introduction of confocal optics which increased its sensitivity to single molecule level during the early 1990s by Rigler and co-workers [2].

The Impact

Along with higher sensitivity the availability of FCS instrumentation with confocal laser scanning microscopes multiplied its utility for biology. Applications include determination of molecular sizes, aggregation states, binding and biochemical kinetics, both *in vitro* as well as *in vivo*.

The Methodology

FCS is a spectroscopic method. The “cuvette” in this case is a diffraction limited spot (Fig. 1). Thus, the reason one uses a microscope is to have a high numerical aperture lens which focuses the beam into a femtoliter sized spot. A welcome side-effect of having a microscope is being able to take an image of the sample for referencing and positioning of the measurement spot (ROI). In FCS the primary read-out is fluorescence intensity over time (fluorescence trace or intensity trace). The fluorescence fluctuations implicitly encode particle numbers (i.e. amplitude of fluctuations) and particle dwell times (i.e. frequency of fluctuations), see Fig. 2. One performs an autocorrelation analysis (“test for self-similarity”) and curve fitting to obtain these parameters quantitatively (Fig. 3, Fig. 4). The geometry of excitation and detection light in the confocal spot roughly follows a three-dimensional normal distribution. By approximating it with a Gaussian function one can find an analytical model for the FCS autocorrelation function (Fig. 5). Its parameters and their physical meaning are summarized in Table 1.

For details on the “anatomy” of an FCS curve, i.e. which processes are observed at what time domain, as well as for a general introduction to the topic, please refer to an online article by Petra Schwille and Elke Haustein [3].

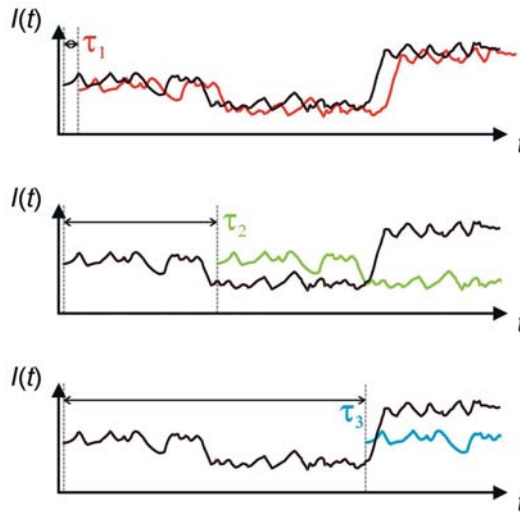


Fig. 3 Principle of autocorrelation. The fluorescence trace gets copied, multiplied by itself and the results summed up. This is done for multiple times, each time shifting the second data set by an increment τ_i (lag time). After small lag times the data is still self similar, resulting in a larger sum (red). Longer shifts mean smaller numbers (green and blue). This technique analyzes the underlying information on the frequency of molecules diffusing through the observation volume.

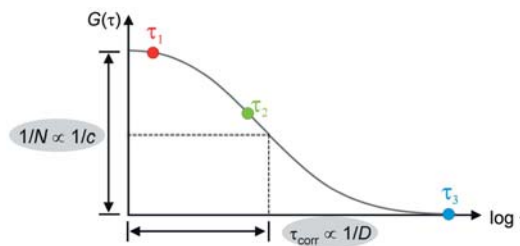


Fig. 4 Autocorrelation function $G(\tau)$ gets plotted over the lag time t . $G(\tau_i)$ representing different lag times is plotted qualitatively from figure 3 (red, green and blue dots). The amplitude at $G(0)$ encodes the inverse of the particle number N . The time at half-maximal amplitude (point of inflection) yields the diffusion time τ_D , also referred to as correlation time. From these numbers one can obtain concentration c and diffusion coefficient D using proper calibration.

$$G_{2D}(\tau) = \frac{\rho}{1 + \left(\frac{\tau}{\tau_D}\right)}$$

Fig. 5 Diffusion model for Gaussian approximation of observation volume. In 2D diffusion (e.g. membranes), x- and y-direction contribute

$$\sqrt{\frac{1}{1 + \left(\frac{\tau}{\tau_D}\right)}}$$

each. In the 3D case a similar term including the structure parameter κ is added. The numerator is a factor containing the particle number.

3D Gaussian Triplet model

$$G_{3D,triplet}(\tau) = (1 - T + T \cdot e^{(-\frac{\tau}{\tau_D})}) \cdot \frac{\rho}{1 + (\frac{\tau}{\tau_D})} \cdot \sqrt{\frac{1}{1 + (\frac{\tau}{\tau_D \cdot \kappa^2})}}$$

Table 1 Parameters of 3D Gaussian Triplet model for data fitting with one molecular species and normal diffusion in 3D.

Parameter	Name	Significance
ρ	Current amplitude	$G(0)$, amplitude contributed by a molecular species
τ_D	Diffusion time	Time molecules spend inside V_{eff}
τ_T	Triplet time	Time molecules spend in dark state
T	Triplet fraction	Fraction of molecules in dark state
κ	Structure parameter	Excentricity of V_{eff} , $\kappa = z_0/w_0$

Equation 1 Effective volume. Size of observation volume relevant to FCS measurements with w_0 as lateral and z_0 as axial extension. Both parameters depend on τ_D and κ obtained by curve fitting of a calibration measurement. Please note that V_{eff} is larger than the confocal volume typically referred to in the literature by a factor of $2^{3/2} \sim 2.8$.

$$V_{eff} = \pi^{3/2} w_0^2 z_0$$

Calibration – from relative to absolute numbers

The two main parameters of interest in FCS measurements are the diffusion coefficient, τ_D , and the number of molecules, N . They directly relate to the diffusion coefficient, D , and the concentration, c , respectively. However, both τ_D and N , are relative numbers influenced by each individual instrument and several experimental parameters. To obtain the absolute numbers D and c is the purpose of instrument calibration.

The effective volume

Both parameters, diffusion time and number of molecules, depend on the size of the observation volume. It shall be referred to here as the effective volume, V_{eff} . Calibration is about determining the size of V_{eff} .

Calibration strategies

Three approaches for determining V_{eff} are described in the literature:

1. Measurement of the confocal volume using fluorescent beads in 3D and fitting a 3D Gaussian function.
2. Preparing a concentration series and plotting N as a function of c . The slope yields V_{eff} .
3. Measurement of known dye with known D . Curve fitting yields τ_D and κ , from which V_{eff} can be calculated.

Each approach has its drawbacks and benefits. For example 1. gives an exact description of the

confocal volume, providing details on how well the 3D Gaussian approximation holds. It is not measured in aqueous solution like the actual measurement. The second approach is model-free, making no assumptions about the geometry of V_{eff} or the diffusion model. It thus contains no information on its shape, it is laborious and may suffer from dark states if no curve fitting is used to estimate N , but it works over a large range of concentrations. The last approach works under conditions very close to the actual FCS measurement, contains some information on the geometry of V_{eff} and can be easily implemented. In the following we shall examine this strategy step by step. For a detailed comparison of all three approaches please refer to [1].

Effective volume obtained by curve fitting

Since this approach is based on curve fitting, the quality of the results depends very strongly on how well the model describes the reality. The strongest assumption made is that of a 3D Gaussian geometry of V_{eff} , as is commonly done in FCS analysis. Misalignment of the system will therefore cause this assumption to be violated. Also, a good signal-to-noise ratio of the autocorrelation is required, because τ_D and κ are both determined from fitting the same data set. This is best fulfilled by bright, photostable dyes in water at a concentration range from 0.1 nM up to 10 nM [1]. The effective volume is then given as in Equation 1.

Step-by-step to effective volume calibration

The first thing we want to do is to prepare a suitable sample. We will start with Alexa 488, since it is photostable, bright and commercially available. We prepare a solution of about 10 nM in water. This means roughly a 1:100000 dilution from a 1mg/ml stock. We also make sure the right filter cube is inserted using a beam splitter at 560 nm and a band pass filter ranging from 500 to 550 nm. We make sure the Argon laser is switched on and run at a tube current of 30 % (1). For all following FCS experiments a 63x 1.2 NA water lens (non-lambda blue) will be used. We launch the SMD FCS wizard.

Adjusting cover glass correction

The first crucial step in FCS is to match refractive indices of immersion medium and sample as well as to adjust the optics to the respective cover glass. This needs to be redone each time the cover glass is changed. Ideally, the cover glass is not changed in between calibration and actual experiment. This could be achieved, for example, by using a glass bottom dish with multiple chambers. One chamber contains the calibration solution and the other chambers contain solutions or cell cultures for the experiments. In step one of the wizard we set the AOTF to 10 % for the 488 line (2), switch the AOBS to reflection (3) and adjust one PMT to detect around 488 nm (4). We use the z-Galvo stage to produce an xz-section of the reflection signal. The goal is to adjust it to maximal brightness and sharpness. We use the following settings: xzy scan mode, 600 Hz scan frequency bi-directional, Zoom 8. The reflection is centered in the field of view. We carefully adjust the correction ring of the lens (5) until maximal brightness is achieved. The Glow OU look-up table can be helpful with that. Once the cover glass is adjusted, we focus about 20 µm into the solution. This could be done using the coordinates on the microscope stand. Set the upper boundary to 0 while the reflection is centered, then focus to + 20 µm.

Adjusting laser intensity

We switch to step two in the wizard (6). AOBS and external port are switched automatically, so we start a test measurement by pressing “RunFCSTest” (7). We acquire one image to position the ROI (8). A potential problem for calibrating the effective volume could be optical

saturation. Optical saturation means that increasing laser intensity does not (linearly) increase fluorescence. For details refer to Gregor, Patra and Enderlein [4]. During a running test measurement, count rates and counts per molecule (= molecular brightness) are displayed (9). Varying the AOTF makes the counts per molecule vary as well. A good rule of thumb is to find the AOTF level leading to the maximal counts per molecule and then using 2/3 of that value. With Alexa 488, 30 % AOTF at 30 % tube current are usually fine. We stop the test measurement and proceed to step three in the wizard (10, 11).

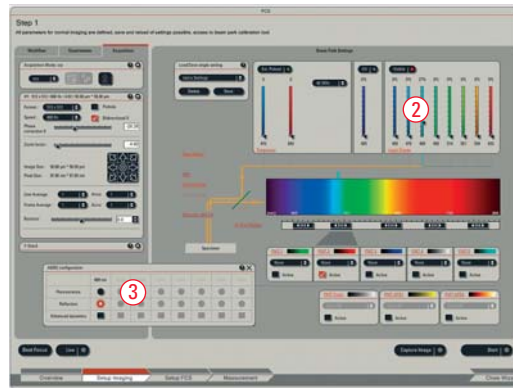


Fig. 6 Step 1 of the SMD FCS wizard. It serves to take images of the sample for positioning of ROIs or, as shown here, to monitor the reflection from the cover glass in xz-mode.



Fig. 7 HCX PL APO 63x/1.20 W CORR CS. The standard objective lens for FCS applications. It also exists as a dipping lens without cover glass correction.

Please Note: This lens is available with a different coating as a “lambda blue” objective. The “lambda blue” lens is not suitable for FCCS with red dyes.

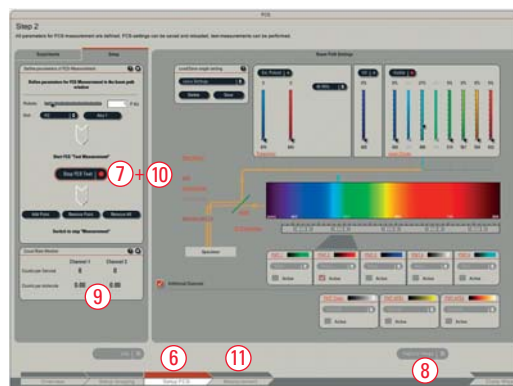


Fig. 8 In Step 2 of the FCS wizard we can adjust the intensity for optimal molecular brightness and test different positions in a sample.

Avoiding artefacts

Certain properties of the dyes under study, experimental conduct or also the FCS apparatus may influence the results considerably. Understanding which artefacts can arise therefore helps to work around them. Artefacts discussed here are detector afterpulsing, dark states, optical saturation, photobleaching.

Detector afterpulsing

Single photon counting means each time a photon hits the detector surface, an electrical pulse is created. Most practical detectors tend to produce a second electrical pulse after the first one with a certain probability. The timing of this leads to a periodicity in the signal on the scale of 10^{-8} to 10^{-7} s. It is observed as a peak in the autocorrelation graph (Fig. 17). In the most simple case, afterpulsing is avoided by omitting it from the fit (excluding everything slower than $0.5 \mu\text{s}$). A more precise strategy is to use cross-correlation or fluorescence lifetime filtering (FLCS) to remove it (see below).

Dark states

Technically, these are not really artefacts but a physical reality of many fluorescent dyes or proteins. Many of those have non-fluorescent quantum states which can be substantially populated at equilibrium or show a complex blinking pattern. Often they are also referred to as the triplet state, because the electronic triplet configuration is the most common contribution to dark states. The average time small molecules spend in dark states is often around a few microseconds. Fluorescent proteins have more complex and multiple dark states. In the case of EGFP they can be approximated with one dark state of about $10 \mu\text{s}$. On this scale dark states are observed in the autocorrelation. Dark states make it difficult to determine $G(0)$ without curve fitting, because they superimpose with diffusion (Fig. 16). As indicated above we can simply introduce two parameters into the model to improve the fit, not caring too much about their absolute values. However, introducing more parameters for fitting requires a better signal-to-noise ratio in the data, which is not always easy to get. Instead, we could characterize the dark state in a separate experiment and introduce it as a fixed number into the model. This would make curve

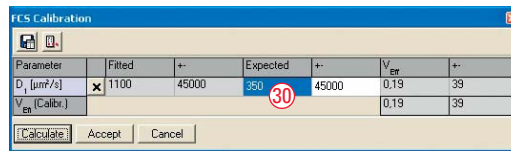


Fig. 13 FCS calibration tool. Information about the molecules under study, such as the diffusion coefficient, is used for volume calibration.

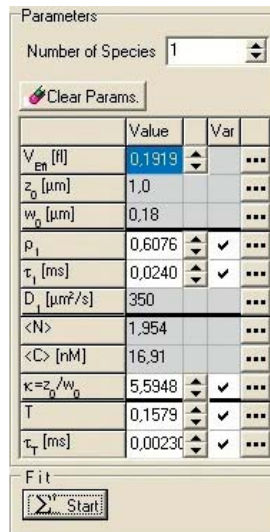


Fig. 14 Result of curve fitting. Parameters with background are part of the diffusion model. The calibrated volume is selected (blue background). Dependent parameters have a grey background and are calculated using fitting parameters and volume calibration data.

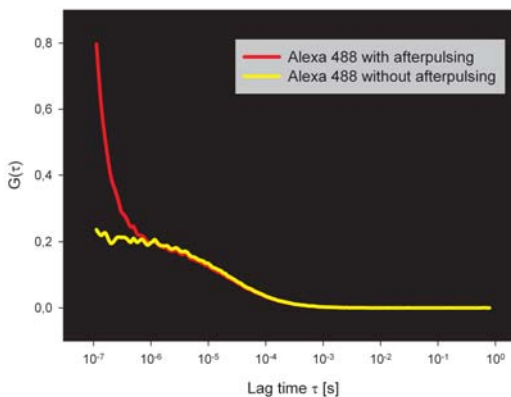


Fig. 15 Effect of detector afterpulsing. This detector property correlates in the range around 10^{-8} to 10^{-7} s (red line). If its contribution is removed, only diffusion and dark states remain (yellow curve).

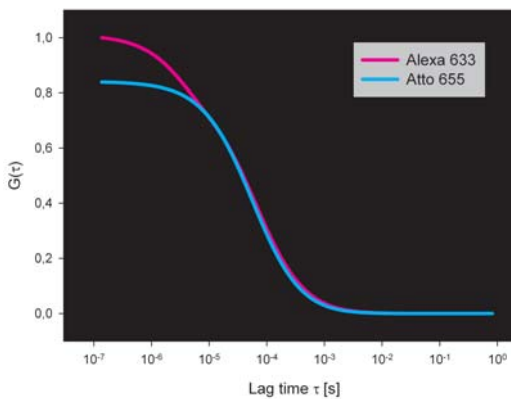


Fig. 16 Effect of dark states. Curve fits of Alexa 633 dye in water (pink line) compared to ATTO 655 dye in water (light blue line). About 20 % of Alexa 633 molecules populate dark states during this measurement, while ATTO 655 is virtually devoid of it. Afterpulsing was removed by FLCS (see below), $G(\tau)$ was normalized to $G(0)$ of Alexa 633.

fitting much more simple. We need to remove afterpulsing from the autocorrelation to get a precise estimate of it.

Measuring dark states by cross-correlation

Since afterpulsing is a statistical process, two detectors will produce afterpulses independently from one another. Conversely, the probability that afterpulsing occurs in two detectors simultaneously is very low. We can use this fact by introducing a 50/50 neutral beam splitter into the detection beam path and using the same band pass filters in both channels. If the same signal is recorded in both channels the cross-correlation contains the same information on dye diffusion and dark states, but not the afterpulsing. For example, Alexa 488 has a triplet time of about 3 μ s. We can now use this as a fixed parameter in the fitting tool. We type in the number and remove the check mark behind it (Fig. 18, (31)). It is recommended to fix the triplet time τ_T , only. Fixing the triplet fraction T is not recommended because the latter depends on experimental parameters such as temperature, pH and excitation intensity.

Fig. 17 Specifying fixed parameters allows one to exploit previous knowledge about the system.

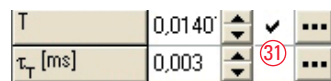


Fig. 18 Opening the FCS trace dialog gives access to re-correlation and time filtering.

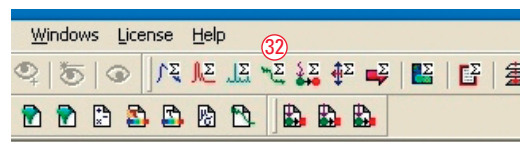


Fig. 19 FCS trace dialog. An additional option with pulsed excitation is FLCS filtering, which allows us to re-correlate the FCS data while de-emphasizing background and detector afterpulsing.

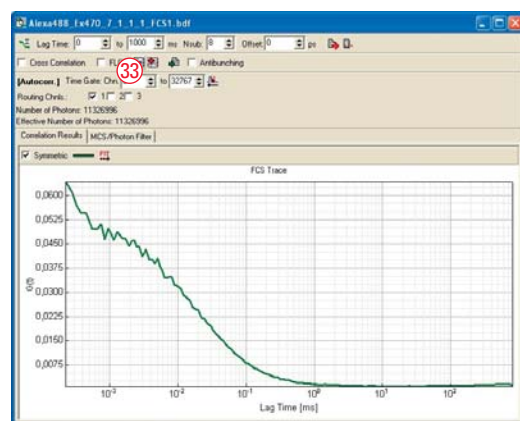
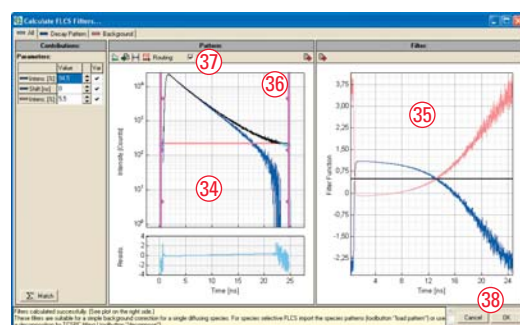


Fig. 20 FLCS filter dialog. The background level is automatically found and the TCSPC decay histogram allows the selection of those photons which stem from actual fluorescence.



Measuring dark states by FLCS

Fluorescence lifetime correlation spectroscopy (FLCS) uses time-resolved fluorescence measurements in more than one way. By using an annotated “raw data” format for storing fluorescence traces, the so-called TTTR format, one is able to interpret the same data set in terms of diffusion by correlation analysis (FCS) as well as in terms of fluorescence lifetime (FLIM). Single-photon counting detectors are used at any rate for FCS, the other pre-requisite is the use of pulsed lasers. For a detailed description please refer to an application note by Picoquant available on-line [6]. Next to quasi-multicolor imaging in one detection channel (not covered here) FLCS can separate contributions from background, scattered light and afterpulsing from fluorescence signals. The latter can be performed as follows. We will again use Alexa 488 dissolved in water. This time we use pulsed laser excitation with 470 nm. Data acquisition is performed as described in steps 1 – 14. After acquisition we open the FCS trace dialog (32). We set Nsub to 8 and choose detection channel 1, as before. We also create an FLCS filter (33). The dialog “Calculate FLCS filters” opens up. On the left hand side the fluorescence decay pattern and background level are displayed (34), while on the right hand side the calculated filter is shown (35). We may need to select the appropriate region using the cursors (36) by moving them slightly inside, away from their initial position. We also choose the appropriate detection channel (37). The filter is calculated in real time and should look something like Fig. 21, (35). The background signal (pink line) should be equivalent to the base line of the fluorescence decay (light blue line Fig. 21, 34). Curve fitting is not necessary for removal of background and artefacts. We press OK (38). This brings us back to the FCS trace dialog. The previously generated photon filter is automatically selected. So, we re-correlate the data (39) and obtain an autocorrelation without afterpulsing and reduced background (40). Performing curve fitting as described earlier (τ_T is determined by the fit) we obtain a triplet time of 2.7 μ s for Alexa 488. For future use of Alexa 488 under comparable conditions we can fix this parameter as shown in Fig. 18. This strategy can be applied to many frequently used dyes or fluorescent proteins which helps to simplify data analysis.

Photobleaching

Photobleaching occurs with most dyes and even more so with fluorescent proteins. As a rule of thumb those dyes which have a lower population of the triplet state tend to be more photostable. Photostability of fluorescent proteins (FPs) has been continually improved [7], but still is mostly inferior to many commercial dyes. Especially with FPs one therefore has to optimize the experiment for small excitation intensity. Photobleaching is observed in the time trace as a fluorescence decrease (Fig. 22 show MCS trace from SPT). This decay is observed in the autocorrelation as well, particularly with lag times around 1 to 10 s (Fig. 24). In some cases it can be helpful to correlate shorter stretches of the time trace and correlate each one individually, because photobleaching does not autocorrelate very much on short time scales. The trade-off is between good signal-to-noise ratio (longer time trace) and bleaching (shorter time trace). Since shorter time traces produce noisier autocorrelation graphs, there is a lower limit to the minimum usable length for autocorrelation. Thus, even better results can be achieved by performing autocorrelation using a sliding average (Malte Wachsmuth, EMBL, Heidelberg, personal communication).

Optical saturation

Photobleaching is not the only process which depends on excitation intensity. There is an intensity range in which the molecular brightness scales about linearly with excitation intensity. That is the most useful range for FCS. At high intensities the molecular brightness remains constant and maximal (or decreases due to photobleaching). This effect is known as optical saturation. In the context of FCS this leads to an apparent increase of the detection volume and an underestimation of the diffusion coefficient [4]. Thus, optical saturation makes the diffusion time a function of excitation intensity and should be avoided (see Fig. 8). A good strategy to detect optical saturation is to vary the excitation intensity and plot the resulting molecular brightness (cpm) as a function of the former. Saturation becomes apparent as non-linearity.

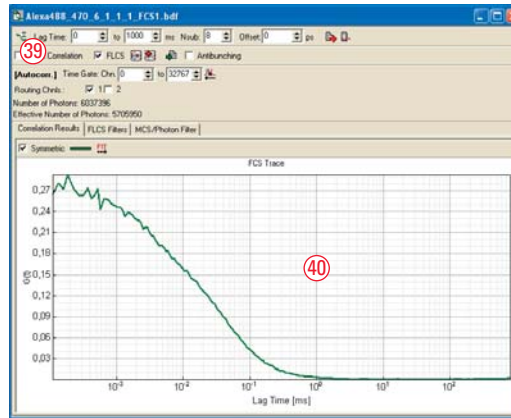


Fig. 21 Alexa 488 autocorrelation after lifetime filtering. In the range of lag times below 1 μs detector afterpulsing is removed.

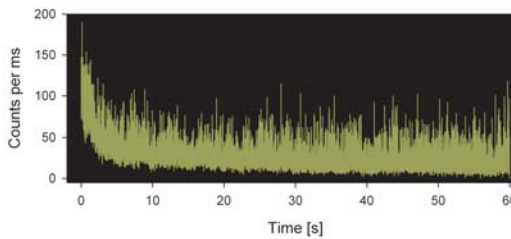


Fig. 22 Arf1-GFP in HeLa cells. Photobleaching is evident as decay of photon counts over time in the MCS trace. Courtesy of Dr. Matthias Weiss, Dr. Jędrzej Szymanski and Nina Malchus, DKFZ, Heidelberg.

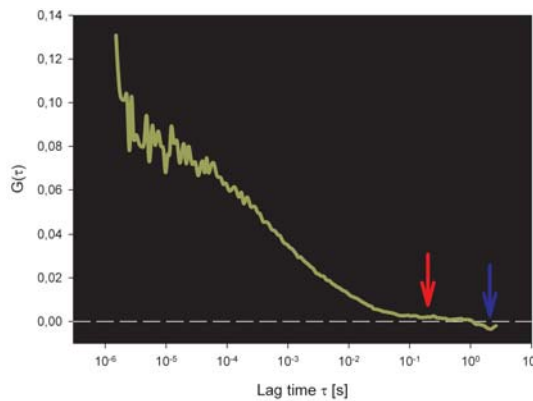


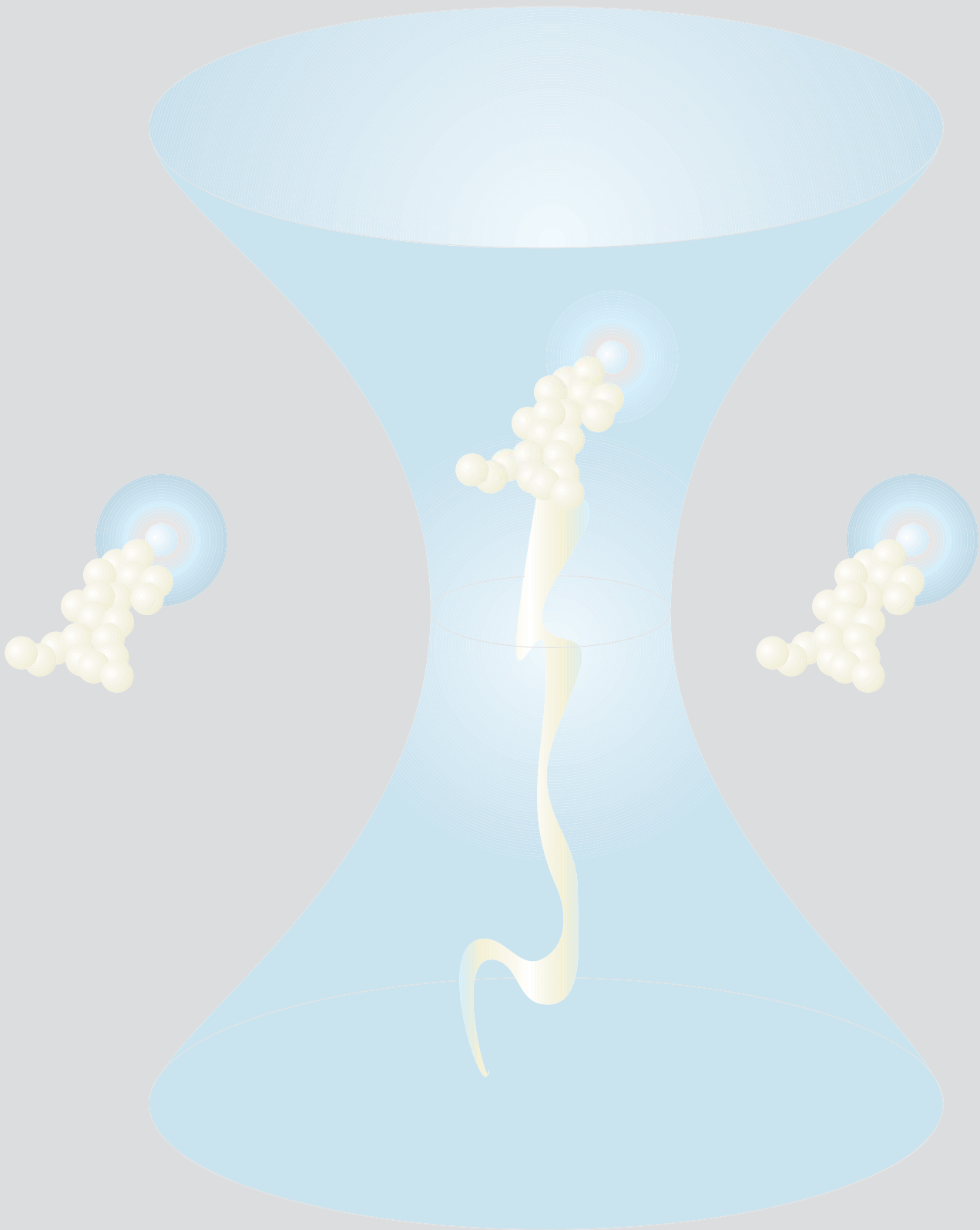
Fig. 23 Arf1-GFP in HeLa cells, autocorrelation. Photobleaching becomes evident in the autocorrelation as fluctuations on the time scale of seconds (blue arrow) and as a non-zero convergence (red arrow). Courtesy of Dr. Matthias Weiss, Dr. Jędrzej Szymanski and Nina Malchus, DKFZ, Heidelberg.

Outlook

FCS is nowadays a standard application, in part, thanks to many technical developments regarding detector sensitivity and laser stability as well as the continuous effort of commercial suppliers to make it accessible. Recent advances of the technique, such as the combination with fluorescence lifetimes in FLCS, show that the technique is still unfolding. Such developments will very likely extend its range of applications in the future.

References

1. Madge, D., Elson, E., Webb, W. W. "Thermodynamic fluctuations in a reacting system – Measurement by fluorescence correlation spectroscopy" *Phys. Rev. Lett.* 29:705-708 (1972)
2. Rigler, R., Widengren J., "Ultrasensitive detection of single molecules by fluorescence correlation spectroscopy." *Bioscience* 3:180-183 (1990)
3. <http://www.biophysics.org/Portals/1/PDFs/Education/schwille.pdf>
4. Gregor, I., Patra, D., Enderlein, J. "Optical saturation in fluorescence correlation spectroscopy under continuous-wave and pulsed excitation" *Chem. Phys. Chem.* 6:164-170 (2005)
5. Rüttinger, S., Buschmann, V., Krämer, B., Erdmann, R., Macdonald, R., Koberling, F. "Comparison and accuracy of methods to determine the confocal volume for quantitative fluorescence correlation spectroscopy" *J. Microsc.* 232:343 (2008)
6. http://www.picoquant.de/_scientific.htm
7. Tsien, R. Y. "Constructing and exploiting the fluorescent protein paintbox (Nobel lecture) " *Angew. Chem. Int. Ed.* 48:5612-5626



“With the user, for the user”

Leica Microsystems

Leica Microsystems operates globally in four divisions, where we rank with the market leaders.

• Life Science Division

The Leica Microsystems Life Science Division supports the imaging needs of the scientific community with advanced innovation and technical expertise for the visualization, measurement, and analysis of microstructures. Our strong focus on understanding scientific applications puts Leica Microsystems' customers at the leading edge of science.

• Industry Division

The Leica Microsystems Industry Division's focus is to support customers' pursuit of the highest quality end result. Leica Microsystems provide the best and most innovative imaging systems to see, measure, and analyze the microstructures in routine and research industrial applications, materials science, quality control, forensic science investigation, and educational applications.

• Biosystems Division

The Leica Microsystems Biosystems Division brings histopathology labs and researchers the highest-quality, most comprehensive product range. From patient to pathologist, the range includes the ideal product for each histology step and high-productivity workflow solutions for the entire lab. With complete histology systems featuring innovative automation and Novocastra™ reagents, Leica Microsystems creates better patient care through rapid turnaround, diagnostic confidence, and close customer collaboration.

• Surgical Division

The Leica Microsystems Surgical Division's focus is to partner with and support surgeons and their care of patients with the highest-quality, most innovative surgical microscope technology today and into the future.

The statement by Ernst Leitz in 1907, “with the user, for the user,” describes the fruitful collaboration with end users and driving force of innovation at Leica Microsystems. We have developed five brand values to live up to this tradition: Pioneering, High-end Quality, Team Spirit, Dedication to Science, and Continuous Improvement. For us, living up to these values means: **Living up to Life.**

Active worldwide

Australia:	North Ryde	Tel. +61 2 8870 3500	Fax +61 2 9878 1055
Austria:	Vienna	Tel. +43 1 486 80 50 0	Fax +43 1 486 80 50 30
Belgium:	Groot Bijgaarden	Tel. +32 2 790 98 50	Fax +32 2 790 98 68
Canada:	Richmond Hill/Ontario	Tel. +1 905 762 2000	Fax +1 905 762 8937
Denmark:	Ballerup	Tel. +45 4454 0101	Fax +45 4454 0111
France:	Nanterre Cedex	Tel. +33 811 000 664	Fax +33 1 56 05 23 23
Germany:	Wetzlar	Tel. +49 64 41 29 40 00	Fax +49 64 41 29 41 55
Italy:	Milan	Tel. +39 02 574 861	Fax +39 02 574 03392
Japan:	Tokyo	Tel. +81 3 5421 2800	Fax +81 3 5421 2896
Korea:	Seoul	Tel. +82 2 514 65 43	Fax +82 2 514 65 48
Netherlands:	Rijswijk	Tel. +31 70 4132 100	Fax +31 70 4132 109
People's Rep. of China:	Hong Kong	Tel. +852 2564 6699	Fax +852 2564 4163
Portugal:	Lisbon	Tel. +351 21 388 9112	Fax +351 21 385 4668
Singapore		Tel. +65 6779 7823	Fax +65 6773 0628
Spain:	Barcelona	Tel. +34 93 494 95 30	Fax +34 93 494 95 32
Sweden:	Kista	Tel. +46 8 625 45 45	Fax +46 8 625 45 10
Switzerland:	Heerbrugg	Tel. +41 71 726 34 34	Fax +41 71 726 34 44
United Kingdom:	Milton Keynes	Tel. +44 1908 246 246	Fax +44 1908 609 992
USA:	Bannockburn/Illinois	Tel. +1 847 405 0123	Fax +1 847 405 0164

and representatives in more than 100 countries